

STATUS OF HIGH POWER TESTS OF NORMAL CONDUCTING SINGLE-CELL STRUCTURES *

V.A. Dolgashev, S.G. Tantawi, SLAC, Menlo Park, CA 94025, USA
Y. Higashi, T. Higo KEK, Tsukuba, Ibaraki 305, Japan

Abstract

We report the results of ongoing high power tests of single-cell standing wave structures. These tests are part of an experimental and theoretical study of rf breakdown in normal conducting structures at 11.4 GHz. The goal of this study is to determine the maximum gradient possibilities for normal-conducting rf powered particle beam accelerators. The test setup consists of reusable mode launchers and short test structures powered by SLACs XL-4 klystron. The mode launchers and structures were manufactured at SLAC and KEK and tested at the SLAC klystron test laboratory.

INTRODUCTION

Our experiments are directed toward the understanding of the physics of rf breakdown in systems that could be used to accelerate electron beams at ~ 11.4 GHz [1]. This means that structure geometries have apertures, stored energy per cell and rf pulse duration close to that of NLC [2, 3, 4, 5] or CLIC [6]. Breakdown rate is the main parameter that we use to compare rf breakdown behavior for different structures [7] at a set of rf pulse parameters (pulse shape, peak power) and 60 Hz repetition rate. In our experiments the typical range of the breakdown rate is from one per few hours to ~ 100 per hour. To date we have tested 9 structures. Below we report the main results of these tests. Further details on these results will be discussed in another publication.

GEOMETRIES

The single-cell standing wave structure consists of three parts: the input coupler cell, the high-gradient middle cell(s), and the end cell [1]. The geometry of the middle cell(s), which are the cells of interest, are based on the geometry of a periodic accelerator structure cell. We list the parameters for these cells in Table 1. In this table H_{max} is the maximum magnetic field, E_{max} is the maximum electric field, Z_0 is 120π Ohm, a is the iris aperture, $\lambda = 26.242$ mm is the wavelength at 11.424 GHz, t is the iris thickness. All field dependent parameters are normalized to 100 MV/m accelerating gradient for a speed of light particle.

The names of the single-cell structures are derived from the names of the corresponding periodic structures plus the manufacturer's name and a serial number. An example of a single-cell structure name is: 1C-SW-A5.65-T4.6-Cu-KEK-#1. Here 1C is the number of high-gradient cells (1 cell in this case), A5.65 is the iris aperture in mm, T4.6 is the thickness in mm, KEK is the manufacturer, and #1 is

the serial number. All the structures were designed with the 2D Finite Element Code SLANS [9] and built at KEK and SLAC. The single-cell standing wave structures we have tested up to now are the following:

- 1C-SW-A5.65-T4.6-Cu-KEK-#1,#2,#3,#4
- (1C-SW-A5.65-T4.6-Cu-TiN-KEK-#1)
- 3C-SW-A5.65-T4.6-Cu-KEK-#1 and #2
- 1C-SW-A3.75-T2.6-Cu-SLAC-#1
- 1C-SW-A3.75-T1.66-Cu-KEK-#1
- 1C-SW-A5.65-T4.6-Choke-Cu-SLAC-#1

With the set of 1C-SW-A5.65-T4.6 structures, we studied the reproducibility of the breakdown behavior with different surface processing techniques and its dependence on pulse shape. We coated the first of these structures with TiN (1C-SW-A5.65-T4.6-Cu-TiN-KEK-#1) to study the effect of a surface with a reduced secondary emission coefficient on the breakdown rate. With the pair of the 3C-SW-A5.65-T4.6 structures, which have three middle high-gradient cells, we studied the breakdown behavior with doubled stored energy for the same surface fields. Then we tested two high shunt impedance structures: 1C-SW-A3.75-T2.6 and 1C-SW-A3.75-T1.66. With these structures we studied the effect of a lower surface magnetic field for the same gradient (compared to 1C-SW-A5.65-T4.6) and a different maximum surface electric field for the same accelerating gradient. We tested a structure with a choke, 1C-SW-A5.65-T4.6-Choke, to study how this means for wakefield damping changes the breakdown behavior.

RESULTS

Of the 10 tests to date, the results for the TiN coated structure and for the structure with a choke were distinctly different from the other 8 tests. First, we will list observations for these 8 structures and then for the two "exceptions".

Typical results

We found that after the initial processing, the breakdown behavior of the copper structures with the same geometries is reproducible from structure to structure and independent of surface quality. At the same time, the pre-test surface preparation (such as high pressure water rinsing and long vacuum baking) effected the initial processing. This is similar to the breakdown behavior of the NLC traveling wave structures.

There is no dramatic difference in the breakdown rate between the single-cell and 3-cell structures for the same pulse shape, even though the stored energy and the input power are ~ 2 times greater. At certain fields and pulse

* This work was supported by the U.S. Department of Energy contract DE-AC02-76SF00515.

Table 1: Parameters of periodic structures normalized for 100 MV/m accelerating gradient.

Structure name	A2.75-T2.0-Cu	A3.75-T1.66-Cu	A3.75-T2.6-Cu	A5.65-T4.6-Choke-Cu	A5.65-T4.6-Cu
Stored energy [J]	0.153	0.189	0.189	0.333	0.298
Q-value [10^3]	8.59	8.82	8.56	7.53	8.38
Shunt impedance [M Ω /m]	102.891	85.189	82.598	41.34	51.359
H_{max} [MA/m]	0.290	0.314	0.325	0.420	0.418
E_{max} [MV/m]	203.1	266	202.9	212	211.4
Losses in a cell [MW]	1.275	1.54	1.588	3.173	2.554
a [mm]	2.75	3.75	3.75	5.65	5.65
a/λ	0.105	0.143	0.143	0.215	0.215
$H_{max}Z_0/E_{acc}$	1.093	1.181	1.224	1.581	1.575
t [mm]	2	1.664	2.6	4.6	4.6
Iris ellipticity	1.385	0.998	1.692	1.478	1.478

widths the 3-cell structure shows obvious run-away behavior: breakdown rate increases with run-time.

For the same field levels and pulse widths, different structures had a different amplitudes of dark current as measured by Faraday cups at the end of the structures. There was no obvious correlation between the dark current amplitudes of these different structures and the breakdown rates.

Figs. 1 and 2 show the difference between a typical low shunt impedance structure (1C-SW-A5.65-T4.6-Cu-KEK-#2) and two high shunt impedance structures (1C-SW-A3.75-T2.6-Cu-SLAC-#1 and 1C-SW-A3.75-T1.66-Cu-KEK-#1). The data shown on the graph were taken with the klystron pulse that was shaped to keep a flat field amplitude inside the structure (after the filling time). The lengths of this flat part are 150 ns for A5.65-T4.6-KEK-#1, 150 ns for A3.75-T2.6-Cu-SLAC-#1, and 200 ns for A3.75-T1.66-Cu-KEK-#1. To date we have tested the reproducibility of the breakdown behavior for the low-shunt impedance structures and we plan to test more high shunt impedance structures with the same geometries.

Fig. 1a) and b) show the maximum surface electric and magnetic fields, calculated based on the shape of the input rf pulse (with similar pulse lengths) and structure parameters. For the same breakdown rate, all 3 structures have similar maximum surface magnetic field and different peak electric fields.

We calculate the accelerating gradient shown in Fig. 2 a) by dividing the maximum surface electric field by the ratio of the surface electric field to the accelerating gradient from Table. 1. We calculate the maximum ‘‘pulse heating temperature’’ in Fig. 2 b) by using the time-dependent magnetic field amplitude [8]. We found that this maximum ‘‘pulse heating temperature’’ is a convenient way to characterize the structures because the breakdown rate is similar for the same ‘‘pulse heating temperatures’’ and different pulse shapes.

As shown on Fig. 2 a) the low shunt impedance and large $a/\lambda = 0.215$ copper structure (1C-SW-A5.65-T4.6-Cu-KEK-#2) ran at gradients above 100 MV/m with ~ 150 ns

flat top pulse with less than 10 breakdowns per hour. The high shunt impedance structure with $a/\lambda = 0.143$ and elliptical iris (1C-SW-A3.75-T2.6-Cu-SLAC-#1) ran at gradients above 140 MV/m with ~ 200 ns flat top pulse with less than one breakdown per hour. The high shunt impedance structure with the same $a/\lambda = 0.143$ and round iris (1C-SW-A3.75-T1.66-Cu-KEK-#1) had similar performance - less than one breakdown per hour above 140 MV/m with ~ 200 ns flat top pulse.

We cut open two low shunt impedance structures (1C-SW-A5.65-T4.6-Cu-KEK-#1 and 1C-SW-A5.65-T4.6-Cu-KEK-#2) for observation. We could see, with a naked eye, the copper grains in the high-gradient middle cell, while in the coupler or end cells the grains were not visible. With a secondary-electron microscope we saw cracks with melted edges between the grains in the area with high magnetic field (see Fig. 3). We did not see these cracks in either the high electric field area or in the input coupler and end cells.

TiN coated and choke structure

The initial conditioning for the structures described above took a few hours with a few vacuum trips. The initial conditioning for the TiN coated structure took a week with numerous vacuum trips. The structure with a choke took 3 days of initial conditioning with multiple chain breakdowns, where the structure was arcing on every pulse at relatively low power. At the end of the initial conditioning, both structures had a high dark current amplitude as measured by the Faraday cups. Unlike in the other structures, the breakdown rate dependence on the rf pulse widths was weak for both the TiN coated structure and the structure with a choke, while the gradient was lower than in the other structures with the same iris shape.

ACKNOWLEDGMENTS

The high power tests of the single-cell structures are conducted at the SLAC Klystron Test Lab with great help from A. Dian Yeremian, James Lewandowski, Chris Pearson, John Eichner, Lisa Laurent, Arnold Vlieks, Chuck Yoneda, John Glenn, John Van Pelt and others.

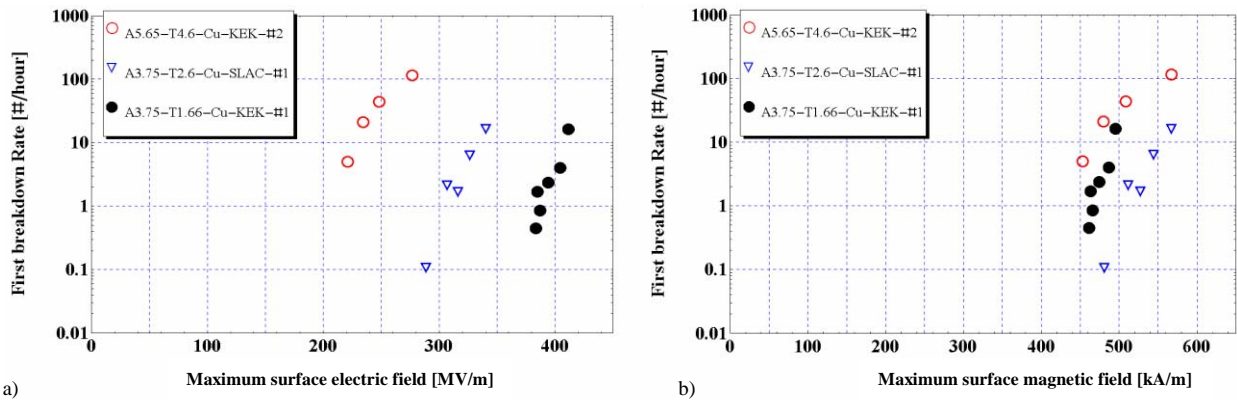


Figure 1: Breakdown rate vs. a) maximum surface electric and b) maximum surface magnetic fields for 3 different single cell structures.

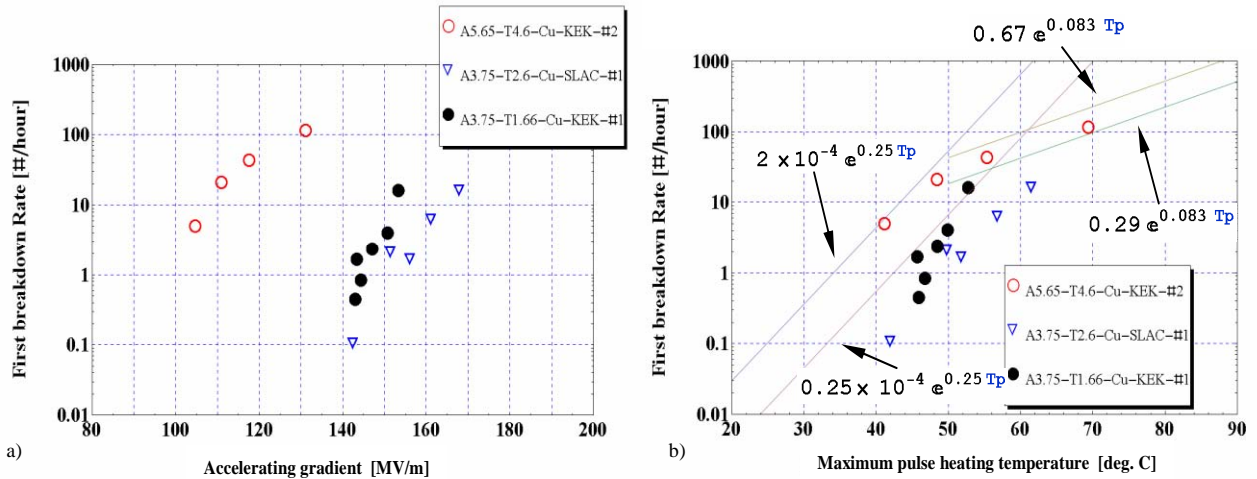


Figure 2: Breakdown rate vs. a) accelerating gradient and b) maximum pulse heating temperature for 3 different single cell structures. The lines in b) outline the boundaries of most of the data for the 1C-SW-A5.65-T4.6 and 3C-SW-A5.65-T4.6 structures. Here T_p is the maximum pulse heating temperature in the cell.

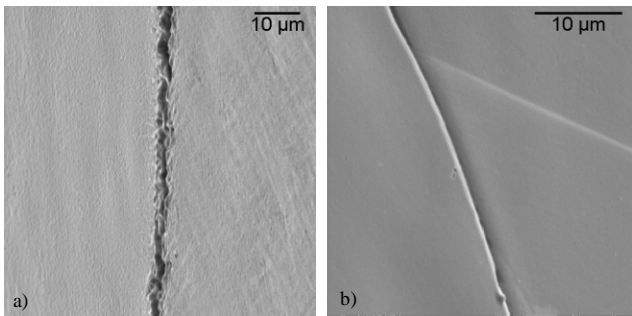


Figure 3: Secondary-electron microscope image of the two grain boundaries: a) in area of high rf magnetic field and b) in area of high electric field of the 1C-SW-A3.75-T1.66-Cu-KEK-#2 structure.

REFERENCES

- [1] V.A. Dolgashev *et al.* SLAC-PUB-11707, Proc. of PAC 2005, Knoxville, Tennessee, 595-599 (2005).
- [2] J. W. Wang, High Energy Phys. Nucl. Phys. **30**, 11 (2006).
- [3] J. Wang and T. Higo, ICFA Beam Dyn. Newslett. **32**, 27 (2003).
- [4] C. Adolphsen, Proc. of PAC 2003, Portland, Oregon, 668-672 (2003).
- [5] V. A. Dolgashev *et al.*, Proc. of PAC03, Portland, Oregon, 1264-1266 (2003).
- [6] Proc. of "The X-Band Accelerating Structure Design and Test-Program Workshop," CERN, Geneva, Switzerland, 18-19 June 2007.
- [7] V.A. Dolgashev *et al.* "High Power Tests of Normal Conducting Single Cell Structures," SLAC-PUB-12956, PAC07, Albuquerque, New Mexico, 25-29 June 2007, pp 2430-2432.
- [8] V. A. Dolgashev, SLAC-PUB-10123, Proc. of PAC 2003, 1267-1269 (2003)
- [9] D. G. Myakishev *et al.*, "An interactive code SLANS for evaluation of RF-cavities and accelerator structures," Proceedings of IEEE PAC01, 1991, San Francisco, Ca, pp. 3002-3004.